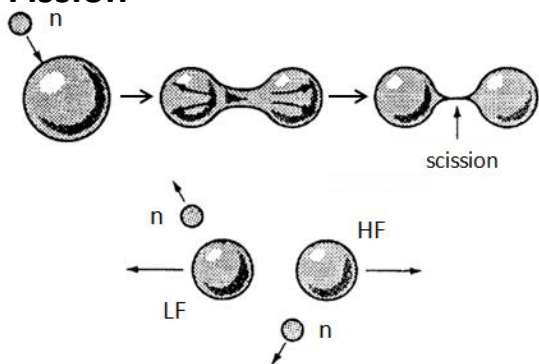Fiesta 2014

Neutron and Gamma Emission in Fission

F. Gönnenwein

University of Tübingen / Germany

Introduction

Fission

Fission was discovered in the reaction $^{235}U(n_{th},f)$ in 1939 (Hahn-Strassmann). A nucleus about to fission is getting deformed until it reaches a critical deformation, the "saddle point". The saddle is in the Liquid Drop Model a point of no return. Beyond the saddle repulsive Coulomb forces between the nascent fragments overtake the surface tension. Eventually the nucleus approaches a dumb-bell configuration with two pre-fragments joined by a thin neck. In the last stage, the "scission stage", the neck ruptures and two separate fragments are set free.

Very heavy nuclei like the Californium isotope ^{252}Cf undergo spontaneous fission. More commonly fission is induced by bombarding a target nucleus with gammas, neutrons or charged particles. In the actinides fission is asymmetric with a light fragment(LF) and a heavy fragment(HF) being formed.

Energetics of the fission process. Example: neutron induced fission

The energy liberated in the primary fission process is

$$Q^* = [M(A_T, Z_T) + M_n + E_n] - [M(A_{LF}^*, Z_{LF}) + M(A_{HF}^*, Z_{HF})]$$

with $M(A_T, Z_T)$ mass and charge of the target nucleus, $M(A_{LF}^*, Z_{LF})$ and $M(A_{HF}^*, Z_{HF})$ the masses and charges of the light and heavy primary fragment before neutron evaporation, and M_n and E_n the mass and incoming energy of the neutron inducing fission, respectively. The energy Q^* is shared between the total kinetic and the total excitation energy of primary fragments, TKE* and TXE, respectively :

$$Q^* = TKE^* + TXE$$

For thermal neutron fission of ^{235}U: $<Q^*> = 195.3(15)$ MeV, $<TKE^*> = 170.5(5)$ MEV, $<TXE> = 24.8(15)$ MeV

At scission most of TKE and TXE is still bound as potential energy V_{Coul} and V_{def}: $TKE^* = E_K^{SCI} + V_{coul}$ and $TXE = E_x^{SCI} + V_{def}$

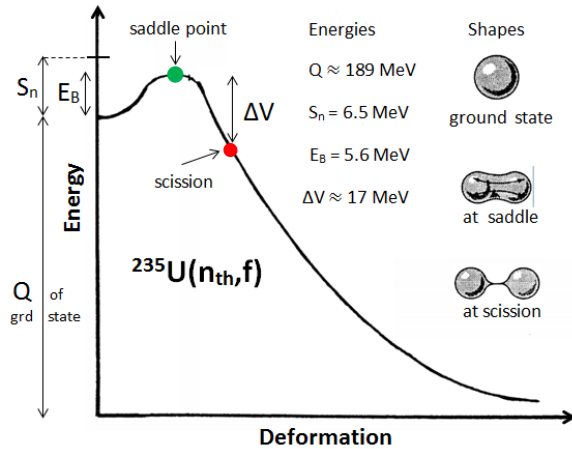## Emission times of Neutrons and Gammas

The excitation energy TXE is evacuated by neutrons and gammas. Prompt neutrons are evaporated by the fragments in times 10^{-18} s to 10^{-14} s. Prompt gammas are emitted after neutron evaporation in times from 10^{-14} s to 1 ms. However, fragments are unstable and only following β-decay become stable fission products. Lifetimes for β-decay range from 1ms to virtually infinity.
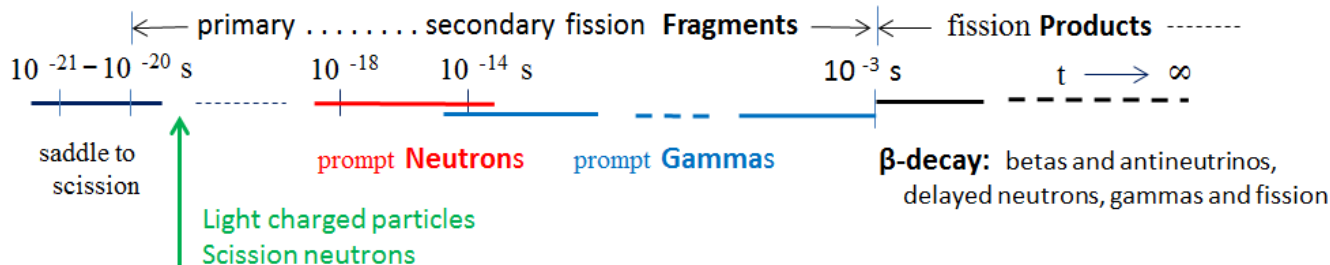
Neutron Emission

Characteristic times in fission

Potential energy versus deformation

saddle point

Energies	Shapes
$Q \approx 189$ MeV	ground state
$S_n = 6.5$ MeV	
$E_B = 5.6$ MeV	at saddle
$\Delta V \approx 17$ MeV	at scission

$^{235}U(n_{th},f)$

scission

Energy

S_n E_B ΔV

Q grd | of state

Deformation

Times

● Time from grd state to saddle in low energy fi $6 \cdot 10^{-15}$ s

● Time from saddle to scission $\approx$ 5 zs

● Neck rupture in $\approx$ 0.5 zs

●Acceleration of FF to 90% of final velocity $\approx$ 5 zs

● Time for relaxation of deformation $\approx$ 5 zs

● Evaporation time for 10 MeV n from FF 10^3 zs

NOTE: 1 zs = 1 zeptosecond = 10^-21 s

Once the saddle has been passed the fission process is very fast, while it takes comparatively a long time to evaporate a neutron. This justifies the assumption that the bulk of neutrons is emitted from fully accelerated fragments. There is however experimental evidence that a fraction of neutrons is ejected right at scission.

Emission Times of Neutrons

Neutrons emitted by the light and heavy group of fragments are rather well separated for neutrons detected along the light and heavy fragment`s direction of motion. In a classic experiment Fraser [1952] exploited this feature to find an upper limit for the times of neutron emission.

The method is based on the comparison of spectra for neutrons emitted by fragments flying in vacuum to spectra from fragments being stopped in the backing of a thin layer of fissile material ($^{233,235}U,^{239}Pu$) being irradiated by slow neutrons. The stopping times of fragments in solid material are very short. In the exponential decrease of their velocity V(t) as a function of time V(t) = V_0 exp$-t/\alpha$ the stopping time constant α is e.g. $\alpha \approx 1$ ps for Al as the stopping medium. In case the neutron emission times are shorter than the stopping times the spectra of un-slowed and down-slowed fragments should be identical. This was tested in experiments sketched for a thin U-foil on a thick Al backing. The assembly was placed in a neutron field.

A

n-detector

neutron

Light FF

Al

235 Uranium

B

neutron

Heavy

FF

n-detector

Al

235 U
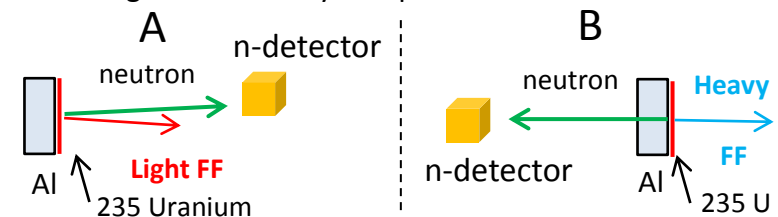
In the schematic drawing only flight paths of those particles being detected are visualized. In part A neutron spectra of un-slowed **light fragments** and in part B spectra from the same **light fragment** but down-slowed are measured. No changes in the spectra could be disclosed. Whence it is concluded that

neutron emission times are shorter than 4·10^{-14} s.

Neutron Multiplicity

a key parameter for assessing neutron emission in fission

Average total Neutron Multiplicities $<\nu_n>$

In low energy fission by far most neutrons are evaporated from fully accelerated fragments. They exhaust the main part of the excitation energy TXE of fragments. To TXE contribute the intrinsic excitation E_X^{sci} accumulated in the descent form saddle to scission and the energy stored as deformation energy V_{def} at scission but converted into intrinsic excitation once the deformation is relaxed after neck rupture:

$$TXE = E_X^{sci} + V_{def}.$$

The neutron multiplicity ν_n is defined as the number of neutrons emitted in one fission event. Of prime interest is the dependence of the total average multiplicity $<\nu_{tot}>$ on the charge and mass of the fissioning nucleus. The table gives some examples for <u>thermal neutron fission</u>.

CN nucleus	230Th	234U	236U	240Pu	246Cm	250Cf
$<\nu_{tot}>$	2.08	2.50	2.43	2.89	3.83	4.08

D. Hoffman 1996
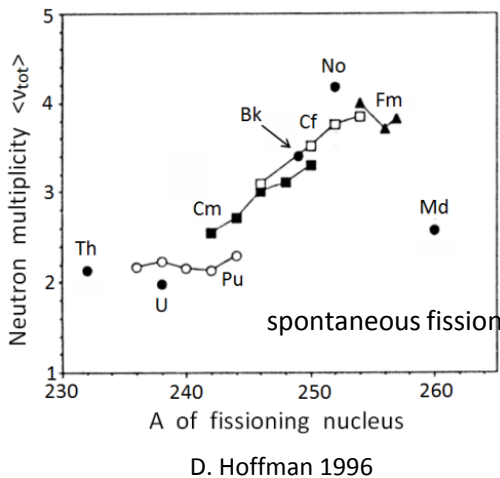
In <u>spontaneous fission</u> of nuclei from Th to Md a similar behavior of $<\nu_{tot}>$ as a function of the mass A of the fissioning nucleus is found (see Fig.). Note that e.g. for ^{240}Pu in (sf) $<\nu>$ = 2.14 whereas in (n_{th},f) $<\nu>$ = 2.89.

Neutron multiplicity *versus* [$<Q_{fiss}>$ − $<TKE>$]

In low energy spontaneous or thermal neutron fission a linear relationship is to be expected between the total number of evaporated neutrons $<\nu_{tot}>$ and the total average excitation energy $<TXE>$ = [$<Q^*>$ − $<TKE>$].

Examples :

^{235}U(n_{th},f): $<TXE>$ = 25(2) MeV thereof 17(1) MeV for neutrons
^{252}Cf(sf) : $<TXE>$ = 36(2) MeV thereof 28(1) MeV for neutrons

D. Hilscher 1992
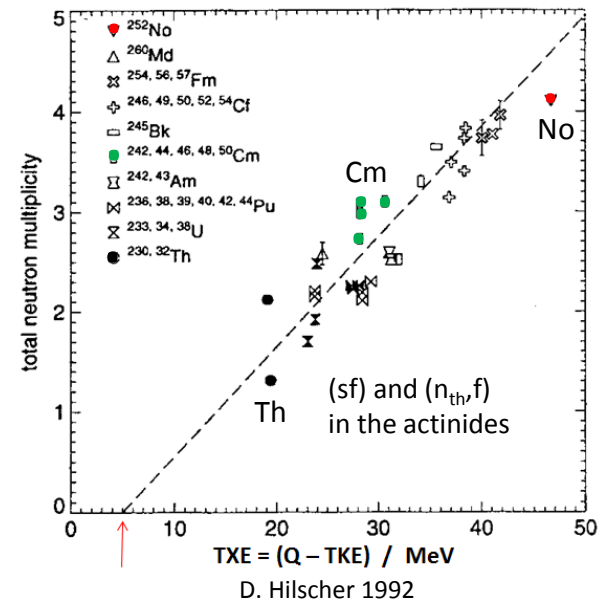
The fit of $<\nu_{tot}>$ to experimental data as a function of $<TXE>$ in the actinides is indeed a straight line as shown in the figure. In the figure there is, however, an offset of about 5 MeV (highlighted by an arrow on the abscissa). The offset is just the excitation energy not exhausted by neutrons but instead by gamma emission.

Distribution of Total Neutron Multiplicity

In low-energy fission (spontaneous fission, thermal neutron induced fission) the distribution of total neutron emission numbers is Gaussian-like, with centers at the average neutron multiplicity $<v>$. Very early in the history of fission research it was remarked that the Gaussians are universal, i.e. identical for all low energy fission reactions (Terrell 1957). The standard deviation σ for all these reactions was given to be σ = 1.08.

$$P(v) = 0.36 \exp[-(v_{tot} - <v_{tot}>)^2/ 2 \sigma^2]$$ with σ = 1.08

Terrell 1957
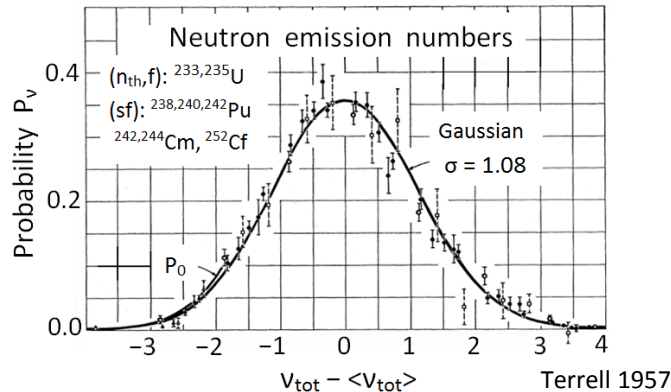
Nowadays it is established that the above rule for $P(v)$ is slightly oversimplified. Only for actinides from U to Cm the variance σ^2 is roughly constant with $\sigma^2 \approx 1.3$ (see table). For the actinides from Cf to No the variances rise significantly (see table).

Of particular interest are the probabilities P_0 for neutron-less fission with $v = 0$. Compare the two characteristic reactions : (n_{th},f) of ^{235}U and (sf) of ^{252}Cf. The average multiplicities are $<v>$ = 2.43 and $<v>$ = 3.76, respectively. Though the averages $<v>$ are close together, the probabilities for neutron–less fission P_0 differ by a factor of 14: P_0 = 3.2 % and P_0 = 0.23 %, respectively.

Variances $\sigma^2(v) = <v^2> - <v>^2$

Distributions are conveniently described by their moments. The first moment, the average, and the second moment, the variance, are of importance. Some examples for variances of total neutron multiplicity $\sigma^2(v_{tot})$ for reactions induced by **thermal neutrons** are given below:

| CN nucleus	234U	236U	240Pu	242Pu
$\sigma^2(v_{tot})$	1.324	1.226	1.347	1.367

The variances as reported by Holden 1988 are seen to be very similar to the earlier findings by Terrell.

Averages and variances of neutron multiplicities for **spontaneous fission** were collected for many reactions by D. Hoffman (1996). Some examples are presented.

Nucleus	240Pu	242Pu	246Cm	252Cf	257Fm	260Md
$<v_{tot}>$	2.14	2.12	2.93	3.76	3.77	2.58
$\sigma^2(v_{tot})$	1.32	1.31	1.31	1.58	2.51	2.57

The rise of the neutron multiplicity variances in the heavy actinides is obvious. Note the irregular multiplicity $<v_{tot}>$ of ^{260}Md otherwise known to undergo bimodal fission.

Total Neutron Multiplicity *vs.* Fragment TKE

Zeynalov 2009
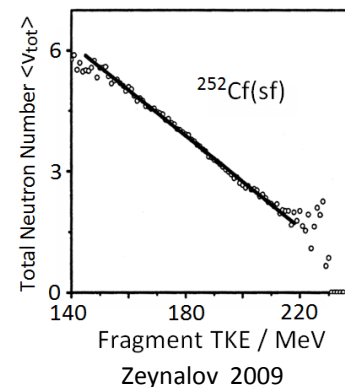
The energy balance in fission reads $Q^* = TKE^* + TXE$. The total excitation energy TXE is drained by n- and γ-emission. For increasing kinetic energy TKE^* the excitation energy and hence the neutron multiplicity $<v_{tot}>$ is hence expected to decrease linearly, as observed. The slope is

$$dv /dTKE = 1 / 12.7 \text{ Mev}^{-1}$$

The saw-tooth of neutron emission

An important result from neutron studies in fission is the discovery that the neutron multiplicity has a peculiar dependence on fragment mass. Plotted as a function of fragment mass the average multiplicity $<v(A)>$ has a saw-tooth like appearance. All experiments agree as to the general trends.

The neutron saw-tooth is best pronounced in low energy fission as demonstrated for ^{252}Cf(sf) and ^{235}U(n$_{th}$,f) in the figures. Shown are the averages $<v(A)>$ as a function of mass A.
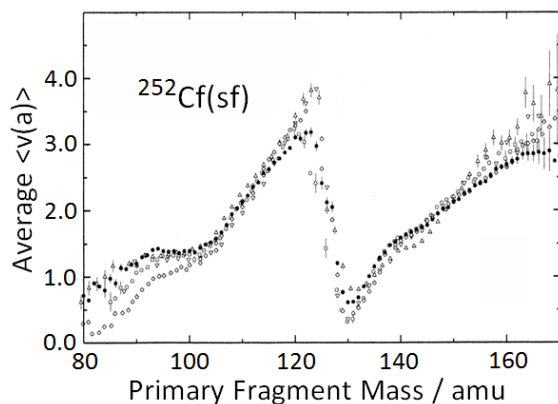
A.S. Vorobyev 2001

- ● Vorobyev 2001
- Δ Zakarova 1979
- O Signarbieux 1972
- ∇ Walsh 1977
- □ Budtz-Jørgensen 1988
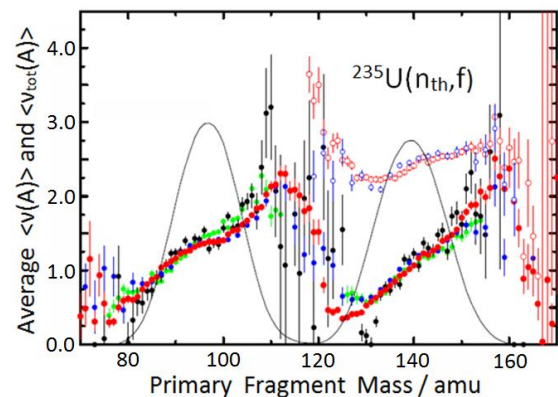
A.S. Vorobyev 2009

For $<v(A)>$
- ● Nishio 1998
- ● Maslin 1967
- ● Müller 1984
- ● Vorobyev 2009

For $<v_{tot}(A)>$
- O Vorobyev 2009
- O Maslin 1967

The saw-tooth phenomenon is intriguing. It is closely linked to the peculiarities observed in the mass-energy distributions of fragments. The minimum neutron multiplicity of $<v(A)>$ for heavy fragment masses near A = 130 is the most startling phenomenon. It is a further evidence for stiff magic fragments close to ^{132}Sn remaining un-deformed at scission and hence carrying no deformation energy. All deformation energy is stored in the shape-distorted complementary light fragment. After shape relaxation the deformation energy is released by neutron evaporation leading to the peak of the saw-tooth $<v(A)>$.
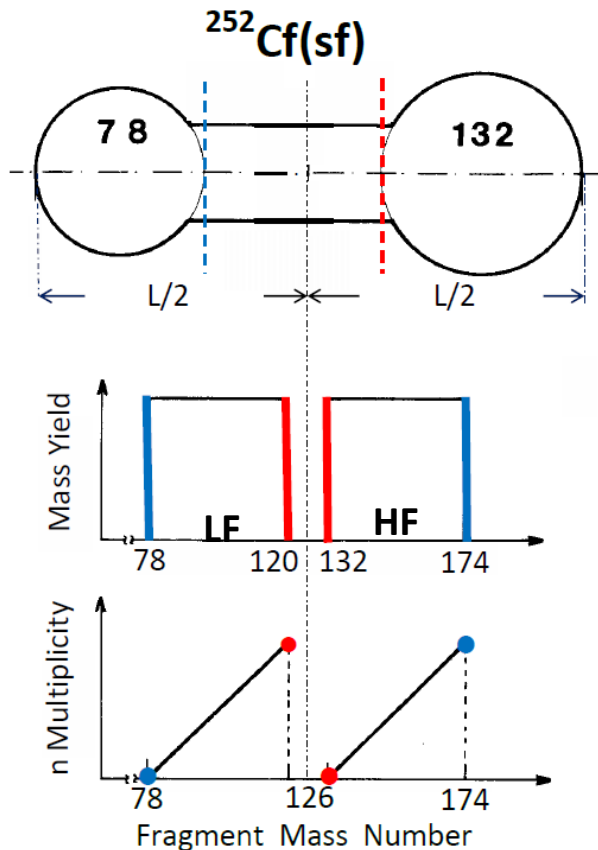
On average the light fragment group as a whole emits generally more neutrons than the heavy fragment group. Calling the group emission numbers v_L and v_H, respectively, some examples for v_L / v_H are collected in the table.

Reaction	^{233}U(n$_{th}$,f)	^{235}U(n$_{th}$,f)	^{252}Cf(sf)
v_L / v_H	1.395/1.100	1.390/1.047	2.056/1.710

From the table it appears that the light group emits about 20-30% more neutrons than the heavy group: v_L /v_H ≈ 1.2-1.3.

The total neutron multiplicity $<v_{tot}(A)>$ for a given mass fragmentation is found by summing the emission numbers $<v(A)>$ of complementary fragments. The total multiplicity is seen in the figure for ^{235}U(n$_{th}$,f) to peak at mass symmetry (open circles). Since the total available energy Q* has to be shared between the kinetic and the excitation energy, Q* = TKE* + TXE, the peak in the total neutron emission, corresponding to a peak of excitation energy, just reflects a kinetic energy dip for fragments near symmetry. This energy dip of TKE is a well known phenomenon.

Schematic yet inspiring model for the neutron saw tooth v(A)

^{252}Cf(sf)

7 8   132

L/2 — L/2

Mass Yield

LF   HF

78   120 132   174

n Multiplicity

78   126   174

Fragment Mass Number

Brosa 1991

The study of fragment mass distributions in low energy fission of actinides has shown that in by far most cases the distributions are asymmetric: a fragment pair consists of a heavy and a light fragment. The mass asymmetry is attributed to the influence of shells in the nascent fragments. It is found that it is highly improbable to break up the spherical Z=50 and N =82 shells of fragments. This is concluded from the observation that nuclei near ^{132}Sn are the lightest nuclei with sizable yields in the heavy fragment group. Similarly, albeit less pronounced, the lightest fragments in the light fragment group are nuclei with masses around 78. This is traced to the spherical magic proton shell with Z = 28 and the magic neutron shell with N = 50.

In a very schematic model of nuclear fission the configuration at scission may hence be visualized like a dumb-bell consisting of two pre-fragments with masses 132 and 78 joined by a long neck (see top part of the figure). For the fissioning ^{252}Cf nucleus there remain 46 nucleons in the neck. To first approximation it is then assumed that the location where the neck is ruptured is distributed randomly along the neck. The stubs remaining after rupture are absorbed by the pre-fragments thereby establishing the final mass of the primary fragments observed in experiment. In the figure (middle part) the schematic mass distribution predicted by the model is on display. The distribution is asymmetric. The limiting mass ratios HF/LF are 132/120 and 174/78.

As a further consequence of the model the deformations of the primary fragments at scission are entirely due to the protruding stubs. The longer the stubs the larger will be the deformations. In the next step the stubs are absorbed by the pre-fragments and the deformation energy relaxes into intrinsic excitation of the fragments. The sharing of the deformation and hence excitation energy between the two fragments is asymmetric. For the mass ratio HF/LF = 132/120 all deformation and excitation energy goes to the light fragment, while for the ratio 174/78 all excitation energy is found in the heavy fragment. Since the lion`s share of the excitation energy is exhausted by neutron evaporation, the model predicts a saw-tooth behaviour of neutron multiplicity v(A) as a function of fragment mass A. The suggested shape of the neutron multiplicity curve in the lower part of the figure conforms surprisingly well with experiment

The investigation both in experiment and theory of the energy spectra of neutrons from fission has a long history and is still going on. To good approximation it is assumed that in low energy fission the bulk of neutrons is evaporated from the fragments having reached their full speed. Fragments reach 90% of their final velocity in $\approx 5 \times 10^{-21}$ s while neutrons are evaporated in times $> 10^{-19}$ s. For example, to evaporate a neutron with energy $E_n = 1$ MeV takes 10^{-18} s.

The starting point for theory is the evaporation spectrum as derived by V. Weisskopf in 1937. The spectrum for 1 neutron emitted in the CM of the moving fragments is:

$$\varphi(\eta) \sim (\eta/T^2) \exp(-\eta / T)$$

with η the kinetic energy of neutrons in the CM of the fragment and T the temperature of the <u>daughter</u> nucleus.

For a cascade of neutrons being evaporated it has been shown that a Maxwell spectrum is a good approach:

$$\varphi(\eta) \sim \eta^{\frac{1}{2}} \exp(-\eta/T_{eff})$$

with $T_{eff} \approx T$ from Weisskopf.

For calculations the temperatures of the two fragments have to be known. To simply set the temperatures of the light and heavy fragment equal to each other does not yield good results. Several recipes how the total excitation energy TXE available is shared between the fragments have been proposed and have to be tested against experiment.

In experiment neutrons and their spectrum is measured in the Lab sytem. For comparison of theory with experiment the CM spectra have do be transformed into the Lab system. The transformation yields a Watt spectrum. Somewhat surprisingly it turns out that also in the Lab a Maxwell spectrum describes well the measured spectra of neutron energy E_n:

$$\Phi(E_n) \sim E_n^{\frac{1}{2}} \exp(-E_n/T)$$

with $\langle E_n \rangle = (3/2)\, T$ and $\sigma^2 = 2\langle E_n \rangle^2 / 3$.

As demonstrated in the figure below, the global spectrum for ^{252}Cf(sf) is well described by a Maxwell distribution. From a fit to the data the temperature is found to be T = 1.42 MeV. This corresponds to an average energy $\langle E_n \rangle = 3/2\, T = 2.13$ MeV.

The peak energy E_p is $E_p = T/2 = 0.71$ MeV. The data are shown both on a linear (a) and a logarithmic energy scale (b) for the neutrons. On the linear scale the exponential decrease of neutron yield for energies E_n in excess of $E_n \approx 2$ MeV is evident. On the logarithmic scale more details of the low energy part of the spectrum come into view.
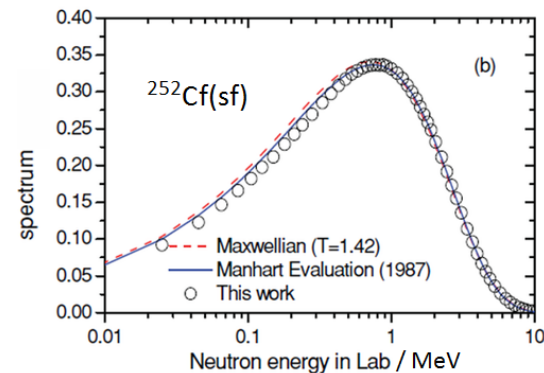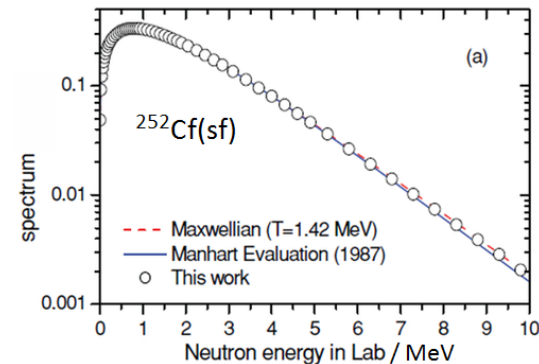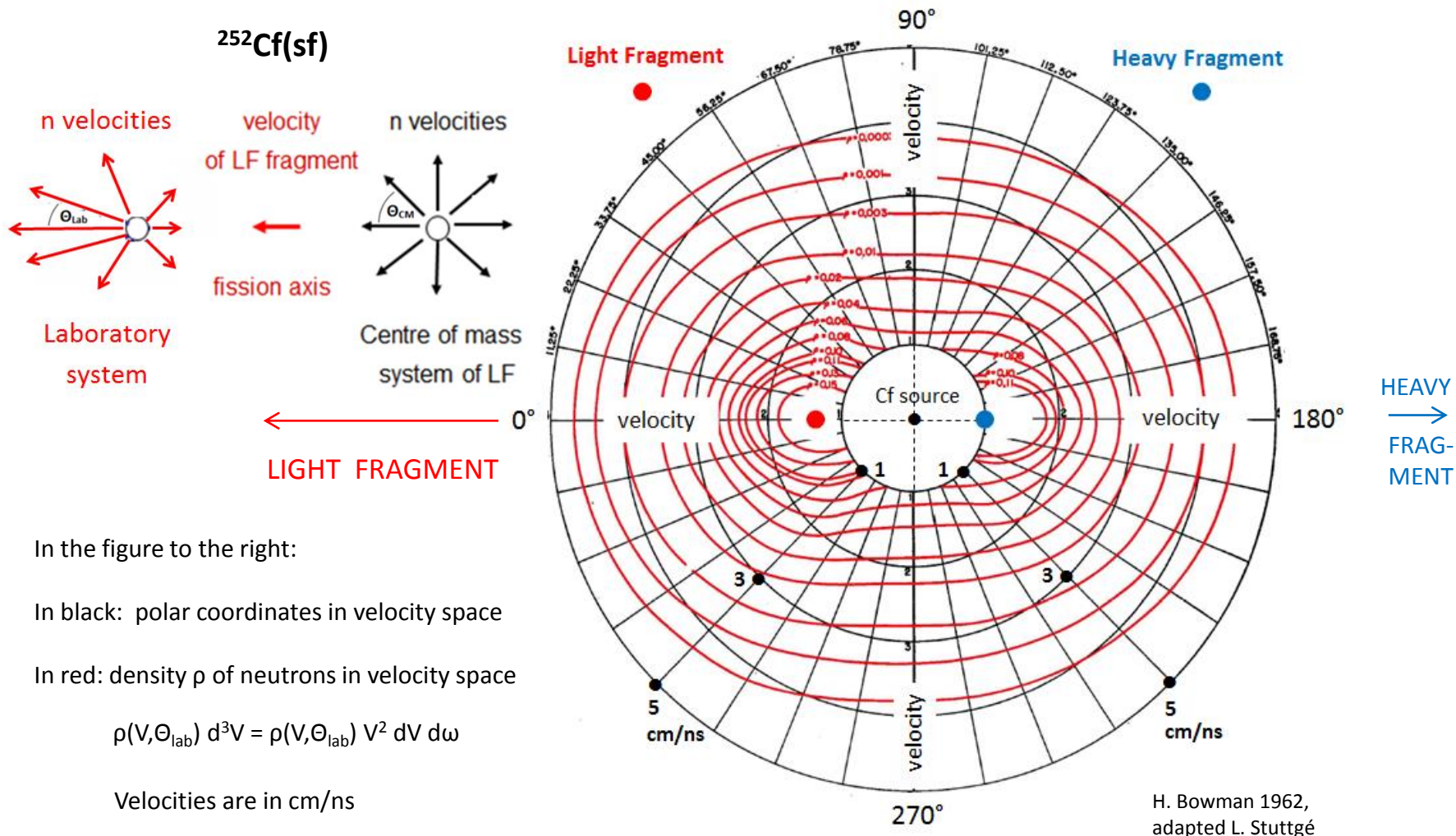

Litaize 2010

The Manhart evaluation (1987) shown in the figure combines the work of several authors. The spectrum often serves as a reference.
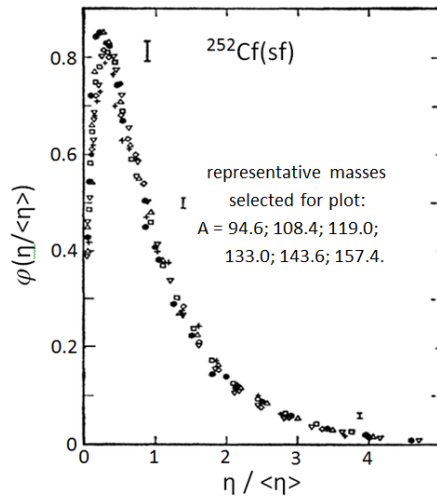
In groundbreaking experiments H. Bowman et al demonstrated in 1962/63 that the bulk of prompt neutrons is evaporated isotropically from fragments having reached their full final speed. Evidence comes from the analysis of velocities and angular distributions of neutrons relative to the fission axis LIGHT ⟷ HEAVY as observed in the LAB system The velocity distribution is markedly non-isotropic: the neutron density as a function of velocity and angle relative to the fission axis is strongly shifted in direction of fragment flight. It is attributed to the isotropic distributions of neutron velocities in the CM systems of fragments with the shift in the LAB system coming about by the vector addition of neutron and fragment velocities. See figures.

^{252}Cf(sf)

In the figure to the right:

In black: polar coordinates in velocity space

In red: density ρ of neutrons in velocity space

$$\rho(V,\Theta_{lab})\, d^3V = \rho(V,\Theta_{lab})\, V^2\, dV\, d\omega$$

Velocities are in cm/ns

H. Bowman 1962,
adapted L. Stuttgé

For the transformation of neutron data measured in the Lab to the CM system of fragments the velocities of fragments have to be known. Velocities are determined by the time-of-flight of fragments over a given distance. In the evaluation both, neutron energies E_n in the LAB and energies η in the CM of fragments are obtained as a function of fragment mass A and total kinetic energy TKE. Hence $E_n = E_n(A,TKE)$ and $\eta = \eta(A,TKE)$. But even for fixed A and TKE the neutron energies are not unique. The reasons are two-fold: particles from an evaporation process cover a range of energies and neutrons emitted in cascade will for each member of the cascade have different energies.

The approach adopted by Bowman (1963) was to search for the CM spectrum $\varphi(\eta)$ in terms of a superposition of evaporation spectra with fixed A and TKE. Assuming that the main sources of fission neutrons are evaporation from the two fragments having reached their full speed, the neutron spectra $\varphi(\eta(A,TKE))$ in the CM are evaluated. A first result obtained is that spectra $\varphi(<\eta(A)>)$ averaged over TKE have the same shape for all masses A. This is visualized i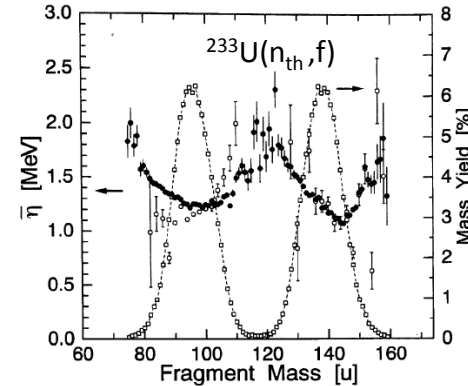n the figure for ^{252}Cf(sf). All spectra $\varphi(<\eta(A)>)$ are subsumed in one universal spectrum $\varphi(\eta)$ when normalized to unity and plotted *versus* the normalized variable $\eta / <\eta>$.
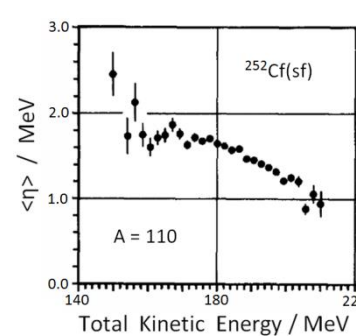
Similar observations were made for the reactions ^{233}U(n$_{th}$,f) and ^{235}U(n$_{th}$,f) which were analyzed in terms of Maxwell distributions by Nishio, 1998. A result is on display

Bowman 1963

for the reaction ^{233}U(n$_{th}$,f). Shown are average energies $<\eta(A)>$ as a function of fragment mass. For comparison also the mass yield Y(A) is shown. For most masses the CM neutron energy $<\eta(A)>$ is between 1.3 and 1.4 MeV. For symmetric and very asymmetric fission the CM energies reach maxim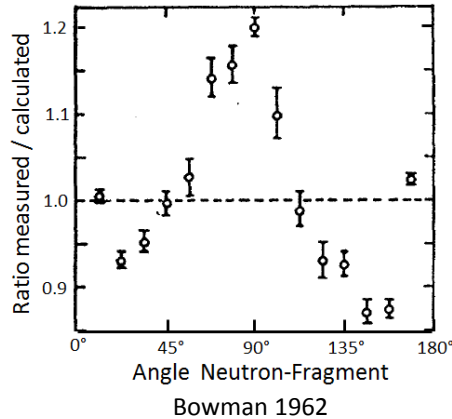a with $<\eta(A)>$ coming close to 2.0 MeV. Remarkably, already back in 1966 H.W. Schmitt found that for ^{235}U(n$_{th}$,f) the total excitation energy TXE = Q*–TKE* becomes large for both, symmetric and super-asymmetric fission, coming close to TXE = 40 MeV.

Nishio 1998

As to the energy dependence of $\eta(A,TKE)$, an example is provided for the mass A = 110 in fission of ^{252}Cf. The neutron energy decreases for increasing kinetic energy TKE of fragments and hence increases with excitation energy TXE.

Budtz-Jörgensen 1988

Though the transformations between neutron spectra in the LAB and the CM systems are rather complex, there is a simple relation for the global averages:

$$<E_n> = <\eta> + <E_f>$$ with E_f = fragment kinetic energy per nucleon

Scission Neutrons *versus* Anisotropic n- Emission in CM system

Already in the pioneering experiments of Bowman *et al.* it was stated that the fit of **angular distributions** with neutrons evaporated isotropically from the moving fragments is only valid within 10-20 %. In particular there are more neutrons emitted at 90° relative to the fission axis than calculated (see plot). It was suggested that about **15%** of all neutrons are ejected isotropically from the composite system being still at rest in the instant of scission.
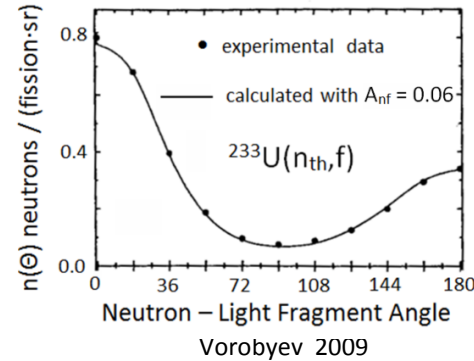

Bowman 1962

Many studies have been devoted to the question whether neutrons emitted isotropically at scission could be the reason for the failure to describe angular distributions of neutrons by two moving emitters. Example: data from $^{235}U(n_{th},f)$ for

Franklyn 1978
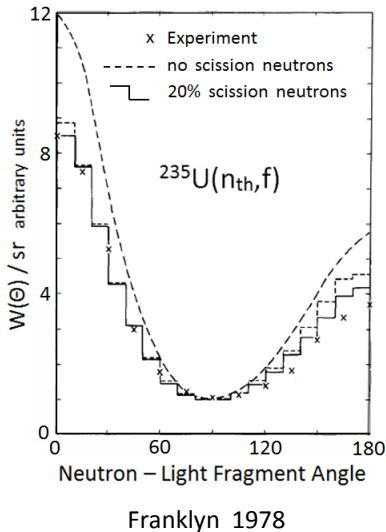
neutron-fragment correlations W(θ) with the angle θ = ∢(n, LF) suggest that up to **20%** of all neutrons could be due to these "scission neutrons".

Note that in direction of the light fragment (θ= 0°) there are more neutrons than in direction of the heavy fragment (θ= 180°) . The reasons are first, that more neutrons are emitted by the light fragment $(v_L/v_H \approx 1.3)$ and second, the kinematical focusing is stronger for the light fragment.
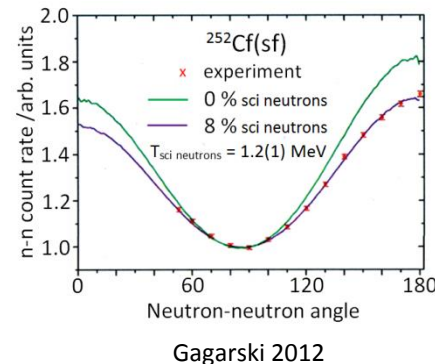
A more recent result is on display for the angular **neutron-fragment correlation** in the reaction $^{233}U(n_{th},f)$. The general appearance of the correlation is similar to the one for $^{235}U(n_{th},f)$ visualized above. But a new feature was intro- in the analysis: neutrons are eva- porated ""anisotro- pically" in the CM system of the fully accelerated frag- ments. The fit is convincing. Claim: less than **5%** of scission neutrons contribute to the total neutron yield.

Vorobyev 2009

A different technique in the search for scission neutrons is to analyze **neutron-neutron correlations**. Coincident neutron-neutron counts from a study with the $^{252}Cf(sf)$ reaction are on display. Taking n-anisotropy into account the assumption of no scission neutrons at all (green curve) does not conform with experiment. Best agreement is reached for a additional contribution by scission neutrons of **8 %** . Remark that at the relative angle 180° more neutrons are found than at 0°. At 180° the two neutrons come from complementary frag- ments while at 0° the two neutrons have to come from one single fragment.

Gagarski 2012

As the preceding discussion has brought to evidence, the abundance or perhaps even the existence of neutrons ejected right at scission is still at issue. The more it is important to discuss from the physics point of view the various possibilities to eject neutrons at the very moment of scission.
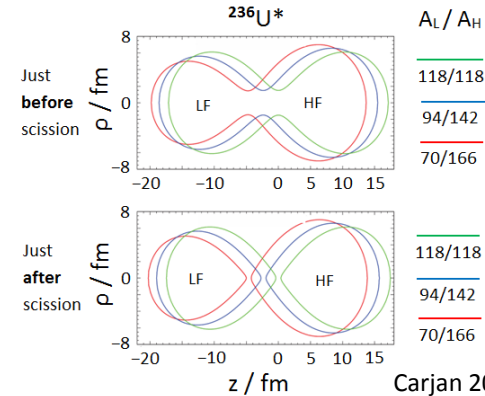
Evaporation of neutrons from the neck near scission is highly improbable since for excitation energies of e.g. 10 MeV it takes about 10^{-18} s. This time is much longer than the times involved in the descent from saddle to scission ($< 10^{-20}$ s) or the acceleration of the fission fragments (90% of final velocity in 5×10^{-21} s). Another process of neutron ejection has to be invoked. When the Bowman experiments discussed above became known in 1962 J.A. Wheeler and R.W. Fuller proposed a quite different mechanism [Fuller 1962]. Attention was given to the extremely short time of about 10^{-22} s taken to rupture the neck at scission. In this short lapse of time nucleons located in the neck can not follow the changes of the potential when the two main fragments start to recede. In this non-adiabatic process the nucleons classically stay where they are and quantum-mechanically their wave functions remain unchanged. But soon after scission the tails of the wavefunctions inside the fragments are aborbed by the fragments and the nucleons are set free. This emission mechanism for light particle emission in fission was first proposed by I. Halpern in 1965.
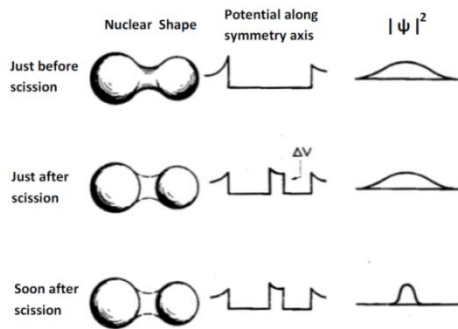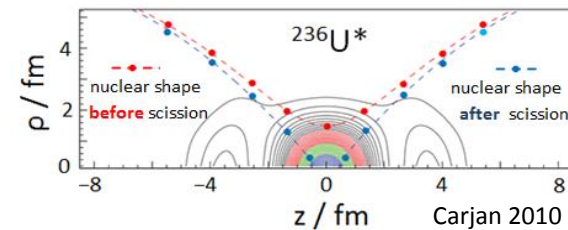

Halpern 1965

Snapshots of the non-adiabatic emission process near scission are shown in the figure to the left. The process may lead to ternary fission in general and to emission of scission neutrons in particular.

In recent times the suggestion by I. Halpern was seized again: the rupture of the neck joining the fragments is followed by a fast absorption of the neck protuberances. In a non-adiabatic process the deformation energy ΔV accumulated from saddle to scission may be converted into intrinsic excitation energy. In the "sudden approximation" the neck just before scission ruptures "instantaneously" yielding two fragments just after scission.

Carjan 2010

The transition is visualized in the figure. The shape of the axially symmetric nucleus is parameterized in cylindrical coordinates (ρ, z).

The probability for the emission of scission neutrons depends on the excitation energy E_X^{SCI}. In the sudden approximation ~ 0.4 scission neutrons appear in fission of $^{236}U^*$. In the figure contour lines of equal probability of emission are sketched for symmetric fission. The emission points are located in the neck region. In the evaluation of neutron data it is assumed that their angular distribu-tion is isotropic. Yet, in view of their place of birth only neutrons ejected at right angles to the fission axis may have a chance to escape. For other angles scattering and absorption of scission neutrons by the near-by fragments may result in a much more complicated pattern.

Carjan 2010

Fission fragments are carrying sizable angular momenta **I**. They are attributed to the collective rotation of deformed fragments. On average their size is $<I> \approx 8\,\hbar$. Intuitively this should lead to anisotropic neutron emission in the CM of fragments, not to be confounded with the kinematical anisotropy in the LAB.

Neutrons evaporated from a rotating nucleus will classically be preferentially emitted in the equatorial plane perpendicular to angular momentum. For fixed spin direction the angular distribution of neutron emission in the CM is described by
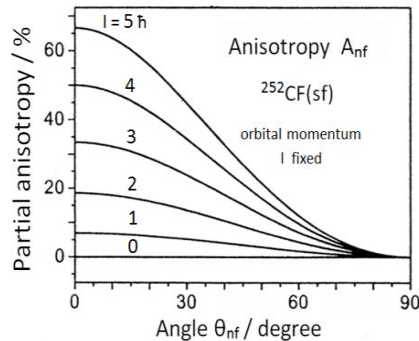
$$W(\theta_{nI}) \sim (1 + a_{nI}\sin^2\theta_{nI})$$
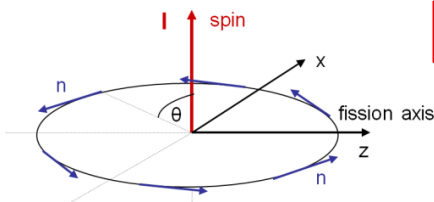
with $\theta_{nI} = \sphericalangle$ (n, fragment spin I)
and the anisotropy
$$A_{nI} = [W(90°) / W(0°)] - 1$$

The spins of fragments are perpendicular to the fission axis. Averaging over all spin orientations perpendicular to the fission axis, an anisotropy for neutrons emerges favoring emission along the fission axis. The angular distribution in the CM reads

$$W(\theta_{nf}) \sim (1 + a_{nf}\cos^2\theta_{nf})$$

with $\theta_{nf} = \sphericalangle$(n, fi-axis)
and the anisotropy
$$A_{nf} = [W(0°)/W(90°)] - 1$$
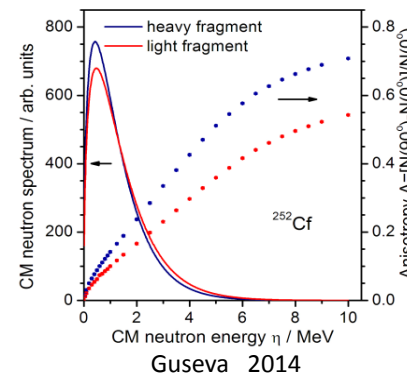Note: $a_{nf} \approx \frac{1}{2} a_{nI}$
Note: the definitions for A_{nf} and A_{nI} are different.

Bunakov-Guseva 2006

The quantal theory of anisotropy as proposed by Gavron (1976) was further developed by Bunakov-Guseva (2006). As shown in the figure, the anisotropy depends markedly on the size of the angular momentum l of neutron emission. As to be anticipated the anisotropy increases with angular momentum l.
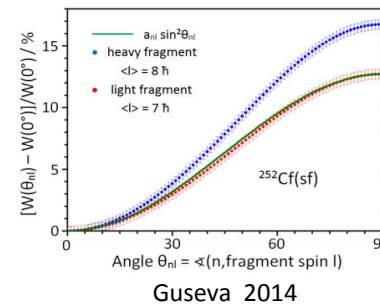
Which neutron angular momenta l are actually showing up depends on the energy η of neutron emission. To any fixed energy η corresponds a probability distribution P(l) of angular momenta l. The angular dependences of neutron emission $W(\theta_{nf})$ relative to the fission axis and $W(\theta_{nI})$ relative to fragment spin **I** are derived for this distribution.

On the other hand the average sizes of fragment spins are known. For any fixed energy η the probability of finding angular momenta l matching the fragment spin has therefore to be calculated. This then allows to calculate anisotropies of neutron emission relative to fragment spin **I**. Anisotropies for the average light and heavy fragment are shown in the figure as a function of CM energy η. For comparison the η-spectrum observed in experiment is inserted in the figure. As to be noticed, for the actual η energies in low-energy fission only rather small anisotropies A_{nI} are to be expected.

Guseva 2014

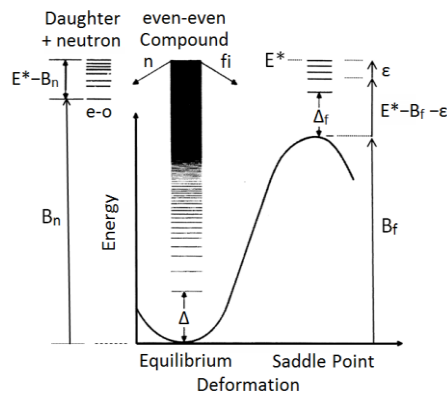Finally the angular distribution $W(\theta_{nI})$ of neutrons relative to spin in the CM of light and heavy fragments is on display in the figure. Only the angle dependent term $a_{nI}\sin^2\theta_{nI}$ is plotted. The functional form $\sin^2\theta_{nI}$ is nicely reproduced. Due to the low η-energies the anisotropy is $A_{nI} \approx 12\text{-}14\,\%$.

Guseva 2014

In the LAB the corresponding $\cos^2\theta_{nf}$ anisotropy relative to the fission axis amounts to $A_{nf} = 6\text{-}7\,\%$.

Irradiating heavy nuclei in the actinides with very low energy neutrons, e.g. thermal neutrons, the absorption of a neutron leads to the always present capture (n,γ) reaction and in case of fissile target nuclei in addition to the fission reaction (n,f). At higher incident energies in the MeV range, following neutron capture fission has to compete with neutron re-emission. This is schematically illustrated in the figure for an e-e compound nucleus. E^* is the excitation energy of the nucleus. In the fission sector to the right B_f, Δ_f, and ε are the fission barrier, the pairing energy gap in the level density of the fissioning nucleus and the kinetic energy in the fission degree of freedom, respectively. The intrinsic energy of excita-

tion at the saddle point is $(E^*-B_f-\varepsilon)$. In the neutron sector to the left B_n is the neutron binding energy while (E^*-B_n) is the excitation energy of the e-o daughter nucleus having evaporated a neutron. The relative probabilities of decay are quantified by the decay widths Γ_f and Γ_n for fission


Vandenbosch-Huizenga 1973

and neutron emission, respectively. The relative probabilities of decay are approximately given by

$$\Gamma_n / \Gamma_f \sim \exp\{- (B_n-B_f)\}.$$

For fissile nuclei like $^{236}U^*$ the difference is $(B_n-B_f) > 0$ (see figure) while for fertile nuclei like ^{238}U one has $(B_n - B_f) < 0$.

At still higher incoming neutron energies in excess of a few MeV both fissile and fertile target nuclei exhibit a peculiar dependence of the (n,f) fission cross section on energy.

A typical example for the fission cross section (n,f) at higher excitation energy is on display for the target ^{238}U.
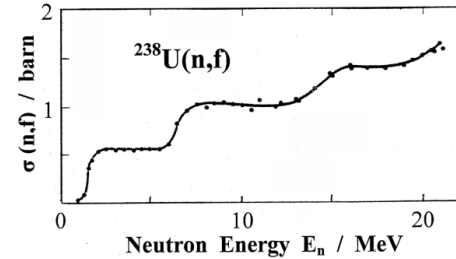
The stepwise increase of the cross section σ(n,f) with incident neutron energy is startling. The explanation is straightforward. For the non-fissile nucleus ^{238}U the fission barrier of ^{239}U is $B_f \approx 6.1$ MeV and thus larger than the neutron binding $B_n \approx 4.8$ MeV gained by neutron capture. For the fission cross section to become sizable the missing 1.3 MeV has to be supplied by the kinetic energy of the incoming neutron. Further increasing the neutron energy the cross section stays constant for about 5 MeV until a second step at ≈ 6.5 MeV indicates that the threshold for a new process has been reached. In the new process a neutron may be emitted from the compound ^{239}U but still enough energy being left to overcome the fission barrier of the daughter


Fréhaut 1989
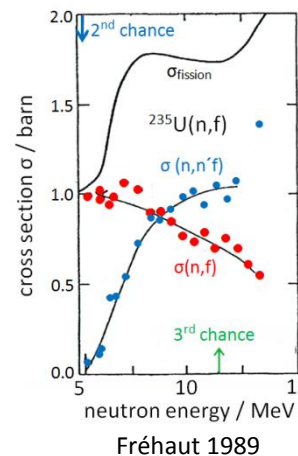
^{238}U. There are thus two processes contributing to fission: "first chance fission" (n,f) and "second chance fission" (n,n´f).

In the figure the onset of 2nd and also 3rd chance fission is marked by arrows for the fissile target nucleus ^{235}U. The contributions of 1st and 2nd chance fission are shown separately. Note the offset of the energy scale.

As shown in foil 04, for spontaneous and thermal neutron induced fission reactions, the total neutron multiplicity $\langle v_{tot} \rangle$ averaged over fragment mass scales with the total excitation energy $TXE = Q - TKE = E_X^{sci} + V_{def}$ being available. Similarly, the multiplicity $\langle v_{tot} \rangle$ rises when the excitation of a specific compound nucleus is raised. Neutron multiplicity is indeed a measure for compound excitation.

Vogt 2009
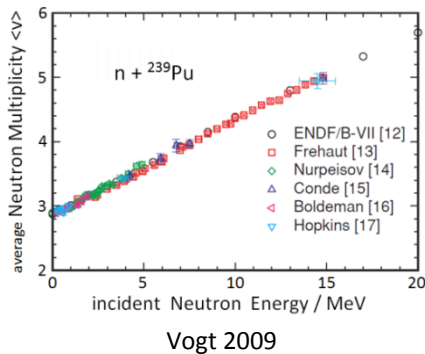
A telling example is provided in the figure for the reaction ^{239}Pu(n,f). In the energy range of 1st chance fission with $E_n = (0 - 5)$ MeV the multiplicity increases with E_n because the temperature of the compound rises. When 2nd and higher chance fission is setting in for $E_n > 5$ MeV

there are besides neutrons evaporated form the fragments also neutrons re-emissioned from the compound nucleus before fission. These are called "pre-scission neutrons".


Ethvignot 2005
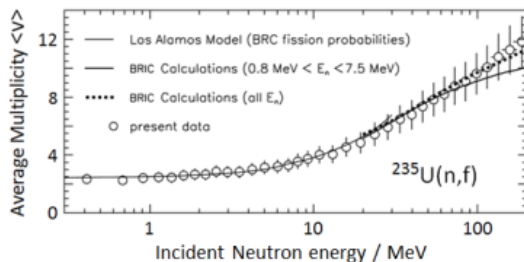
As the figure for the ^{235}U(n,f) reaction indicates, neutron multiplicity rises continuously up to very high incident neutron energies. At 200 MeV neutron energy five times

more neutrons are produced than with reactor neutrons. It could further be proven that most neutrons (85 %) are either evaporated from the fragments or emitted from the CN nucleus as pre-scission neutrons. Only 15 % are ejected by pre-compound processes.

It has to be pointed out that this type of data are of importance in the design of hybrid reactors where the fission reaction is driven by a proton accelerator of high energy (up to 1 GeV) producing neutrons of high energy via the (p,n) reaction. Hybrid reactors would allow to burn the minor actinides present in the nuclear waste of standard power reactors.

An interesting observation is the change of the saw-tooth like shape of multiplicity $\langle v(a) \rangle$ when the excitation of the fissioning nucleus is raised from low to higher energies. The changes corroborate the interpretation of the minimum $\langle v(A) \rangle$ near ^{132}Sn as being due to shell effects. Shell effects are known to become weaker at higher excitation energies. This is indeed observed in the growth of multiplicity $\langle v(A) \rangle$ near ^{132}Sn for the reaction ^{237}Np(n,f) visualized in the figure. Increasing the incoming neutron energy the excitation is raised from 7 to 12 MeV and magic nuclei become more easily deformable. After scission the deformation energy relaxing into intrinsic excitation leads to an increased neutron evaporation from fragments near A = 132 [Naqvi 1986]. While in the light mass group the multiplicity remains virtually constant, the


Hilscher-Rossner 1992
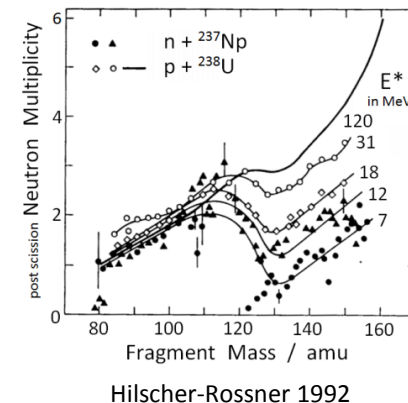
increase in the heavy group smoothes out the saw-tooth until in the reaction ^{238}U(p,f) at E* = 120 MeV a LDM-like behaviour is reached. Experiments are well described by theory [Ruben 1991, Schmidt 2010]

Most neutrons are evaporated in times smaller than a few 10^{-14} s. These are called prompt neutrons. A second fraction of neutrons is showing up at much later times starting at about 1 ms after fission. These late neutrons are therefore called "delayed neutrons".

   After prompt neutron emission the "primary" fragments have become "secondary" fragments. As a rule these latter fragments are still too n-rich and hence unstable. To reach the stability line of the nuclide chart they undergo β^- -decay. The β-decay is induced by the weak interaction and the corresponding reaction times are long. For secondary fragments showing up in fission the β^--decay times range from $\sim$ 1 ms to   times much longer than the age of the universe. For many of the fragments β^- -decay leads in the daughter nucleus to excitation energies in excess of the neutron binding energy. In these cases – besides delayed gammas – delayed neutrons may be emitted.

   In emission of delayed neutrons the nuclei involved are the n-precursor fragment $^A_Z X_N$, following β-decay the neutron emitter $^A_{Z+1} Y_{N-1}$ and following n-emission the final product $^{A-1}_{Z+1} Y_{N-2}$ + **n.** The level schemes illustrate cases favorable for the emission of delayed neutrons.
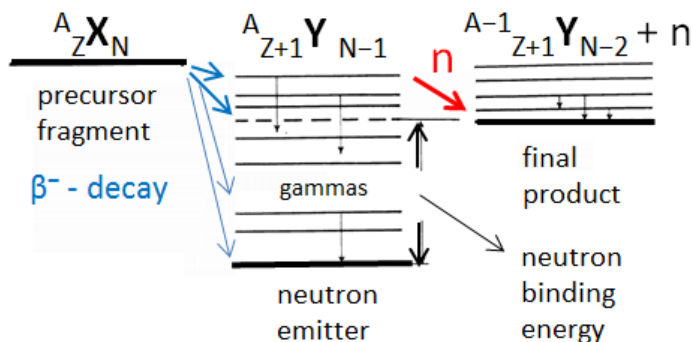
The number N_β of β-decays for thermal neutron induced fission of actinides is N_β = 6.0 $\pm$ 0.5. Among the fission products about 300 nuclei are precursors to emission of neutrons. Most delayed neutrons appear within 1 min after fission. They are of crucial importance for the safe operation of power reactors. To simplify the analysis they are lumped together into 6 groups according to their half-lives $T_{1/2}$. Delayed neutron data for $^{235}U(n_{th},f)$ are given in the table. The characteristic parameters are the half-lives $T^{1/2}$, average neutron energies $<E_n>$ and probabilities P_k in % for the six groups labeled k. They are shown in the table:

k	$T_{1/2}$ /s	E_n/MeV	P_k /%
1	53.0	0.41	3.5
2	21.6	0.47	18.1
3	5.3	0.44	17.3
4	2.3	0.56	38.7
5	0.83	0.52	15.6
6	0.25	0.54	6.6

D.E. Cullen 2004

Averaged over all groups the half-life for delayed neutrons from thermal fission of ^{235}U is

$$<T_{1/2}> = 9.0 \pm 1.0 \text{ s}$$

Energy spectra of delayed neutrons are parameterized as Maxwellians

$$P(E_n) \sim E_n^{1/2} \exp(-E_n/T) \text{ with } <E_n> = 3T/2$$

The average $<E_n>$ of the energies on display in the table is

$$<E_n> = 0.51 \text{ MeV}$$

For thermal neutron fission of ^{235}U and ^{239}Pu the ratio

$$\beta = v_{del}/v_{tot} \text{ with } v_{tot} = v_{prompt} + v_{delayed}$$

is β = 0.65% and β = 0.24%,   respectively.

Gamma Emission

Following scission and the relaxation of their deformation the fission fragments are as a rule highly excited with average total excitation energy TXE ≈ 24 MeV and ≈ 36 MeV for (n_{th},f) of ^{235}U and ^{249}Cf, respectively. This energy is evacuated by emission of neutrons and gammas. First prompt neutrons are emitted up to times of about 10^{-14} s. When the excitation energy has fallen behind the neutron binding energy gamma emission takes over. The energy left behind per fragment is $\geq \frac{1}{2}S_n$ with S_n the neutron binding energy. Per fission event one therefore expects to observe a total prompt gamma energy $E_{\gamma pT} \geq S_n$. In a model the average **residual excitation energy** left, when neutron evaporation has stopped, was calculated for two reactions: $^{235}U(n_{th},f)$ and $^{238}U(sf)$. The results in the figure show that the energy left for gamma emission decreases for increasing neutron multiplicity ν. For the average multiplicity <ν> = 2.43 in $^{235}U(n_{th},f)$ this energy is

≈ 5 MeV. This energy agrees with binding energies S_n as calculated from mass tables for thermal neutron fission of ^{235}U. Examples for S_n are given in the figure.
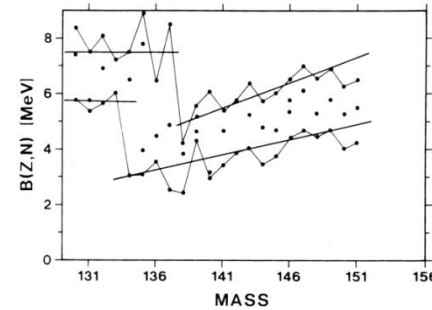

Neutron binding energies for FF from $^{235}U(n_{th},f)$.
Heavy FF group.
Straight lines are smoothed max and min binding energies S_n.

Knitter 1991

However, in the total time and energy window of prompt gammas, the total average γ-energy $<E_\gamma>$ could be larger and come close to $<E_\gamma> ≈ 8$ MeV (see table below).

Emission times for gammas cover a large range from about 10^{-14} s up to 1 ms. At the shortest times of 10^{-14} s gamma emission competes with neutrons. At the longer times of roughly 1 ms after fission the fastest β-decays of fragments start and the fragments become fission products. Also the products may emit gammas. They are called delayed gammas in order to distinguish them from the prompt gammas emitted by fragments. The time for turnover from prompt to delayed gammas is usually taken to be 1 ms.
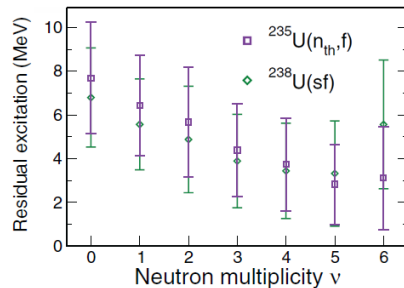
Residual excitation energy for events with given neutron n multiplicity ν in $^{235}U(n_{th},f)$(squares) and $^{238}U(sf)$ (diam.)
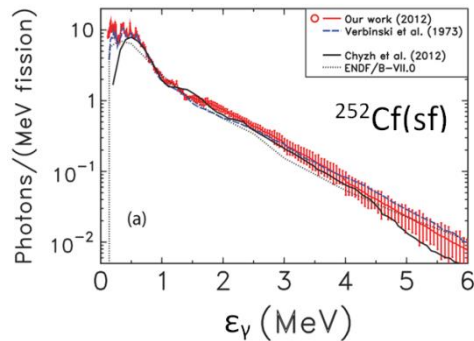
R. Vogt 2011

^{252}Cf(sf)

Fiesta 2014-18
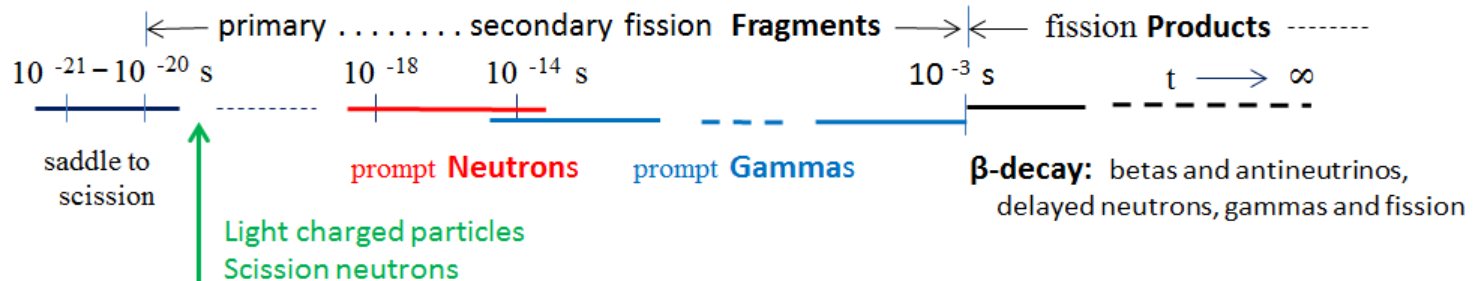
^{235}U(n$_{th}$,f)

Compared to many other topics in fission, gamma emission has not been much studied. Measurements are difficult because γ-energies range from a few tens of keV up to 10 MeV and the emission times vary from 10^{-14} s up to 1 ms. Most data have been taken for times within 10 ns after fission. The best studied reactions up to date still are ^{252}Cf(sf) and ^{235}U(n$_{th}$,f).

Of prime interest are the energies ε_γ of individual photons and their multiplicity M$_\gamma$. In recent comprehensive studies the gamma emission from ^{252}Cf(sf) was studied and compared to data taken 40 years earlier. Gamma spectra were taken by dif-

ferent detector types:
Blue: NaI(Tl); 1973
Red: LaBr$_3$:Ce; 2013
Curve: BaF$_2$; 2012
For the bulk of quanta:
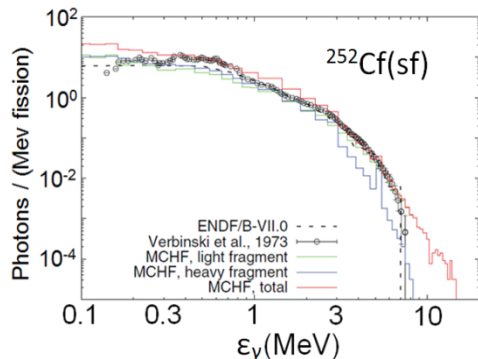0.3 < E$_\gamma$ < 1.0 MeV.
Time window: < 10 ns.

Blue: Verbinski 1973
Curve: Chyzh 2012
Red: Billnert 2013,

The gamma-spectrum is well described by theory as brought to evidence in the figure for the reaction ^{252}Cf(sf). Plotted are


Becker 2013 theory

experimental results (circles Verbinski 1973), evaluated data (dotted ENDF/B-VII.0) and theoretical results (histograms for light and heavy fragment, and total from Monte-Carlo Hartree-Fock model).

The gamma spectrum observed in the standard reaction ^{235}U(n$_{th}$,f) is not much different from the one in (sf) decay of ^{252}Cf. In going from gamma energies ε_γ near ε_γ = 1 MeV
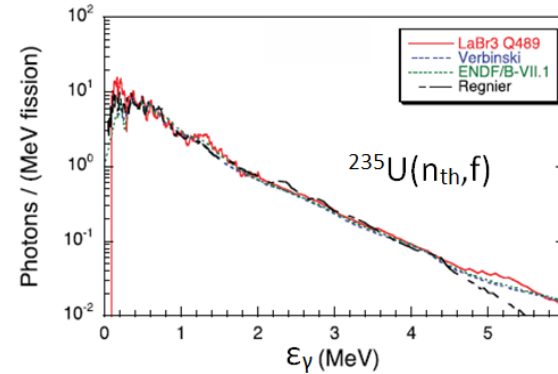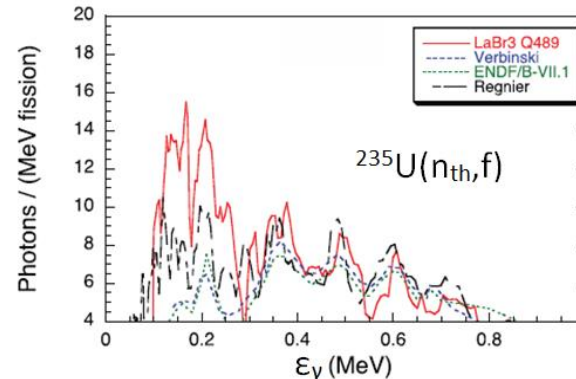

A. Oberstedt 2013

Detectors:
Blue: NaJ(Tl)
(Verbinski 1973)
Red:LaBr$_3$:Ce
(Oberstedt 2013)
Dashed: theory
Regnier 2013

to ε_γ = 6 MeV the emission probability decreases smoothly exponentially by 4 orders of magnitude. Only at low energies ε_γ < 1 MeV a fine structure shows up.

This structure becomes convincing in a zoom for gamma energies below 1 MeV. The structure was already observed in 1957 [Voitovetskii] , established in 1973 [V. Verbinski] and corroborated with high resolution 40 years later. The structure is attributed to collective rotational levels of (e,e) fission fragments.

A. Oberstedt 2013

Detectors:
Blue: NaJ(Tl)
(Verbinski 1973)
Red:LaBr$_3$:Ce
(Oberstedt 2013)
Dashed: theory
Regnier 2013

Total Prompt Gamma Energy E_γ

Fréhaut 1989
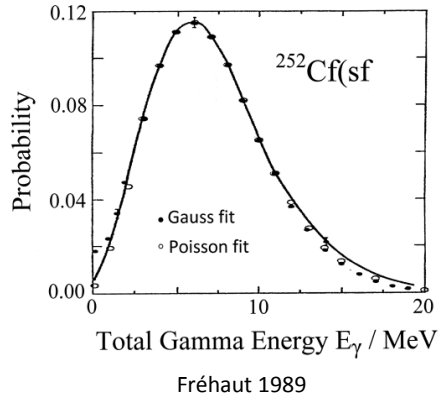
The distribution of total prompt gamma energy E_γ set free in ^{252}Cf(sf) is shown in the figure. The energy was accumulated during 30 μs after fission in a NaI detector. On average the energy is quoted to be

$<E_\gamma>$ = 7.1 MeV.

The contribution by gammas emitted beyond 30μs is negligibly small.

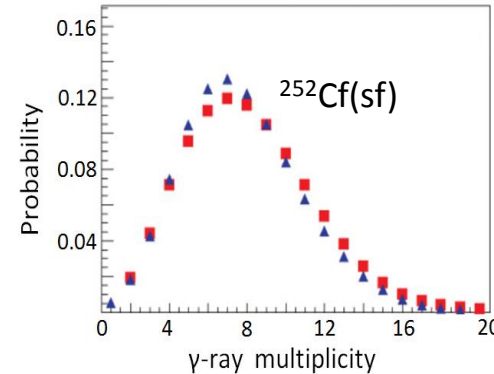## Comparison of Results on Gamma Energies

Results on gamma energies from different experiments are delicate to compare because they differ either in the energy range ΔE of gammas or the time window Δt of emission analyzed. Compared are the multiplicity M_γ, the single photon energys ε_γ and the total gamma energy release E_γ.

^{235}U(n_{th},f)	ΔE MeV	Δt ns	$<M_\gamma>$	$<\varepsilon_\gamma>$ MeV	$<E_\gamma>$ MeV
Verbinski 1973:	0.14-10.0	10	6.7(3)	0.97(5)	6.5(3)
Chyzh 2013:	0.15-9.5	100	6.95(30)	1.09	7.57
Oberstedt 2013:	0.1-6.0	~ 10	8.19(11)	0.85(2)	6.92(9)

^{252}Cf(sf)	ΔE	Δt	$<M_\gamma>$	$<\varepsilon_\gamma>$	$<E_\gamma>$
Verbinski 1973:	0.14-10.0	10	7.8(3)	0.88(4)	6.84(30)
Skarsvag 1980:	> 0.114	12	9.7(4)	0.72	7.0(3)
Chyzh 2012:	0,15-9.5	10	8.15	0.96	7.8
Billnert 2013:	0.1–6.0	<1.5	8.3(1)	0.80(1)	6.64(8)

Note: the smallest ε_γ energies of single gammas from fragment nuclei are close to 100 keV. By comparison: the energies of K_α X-rays are ~ Z^2 with Z the atomic number; $E_{K\alpha} \approx$ 73 keV for Pb.

Gamma Multiplicity M_γ

The gamma multiplicity for thermal neutron induced and spontaneous fission of ^{252}Cf are vey similar. An example is presented for ^{252}Cf(sf). On average there are $<M_\gamma>$ = 8.14(40) gammas emitted. The multiplicity extends up to M_γ = 20

Red: Chyz 2012
Blue: Verbinski 1973

Dependence of Mean and FWHM of Total Gamma Energy E_γ on Multiplicity M_γ
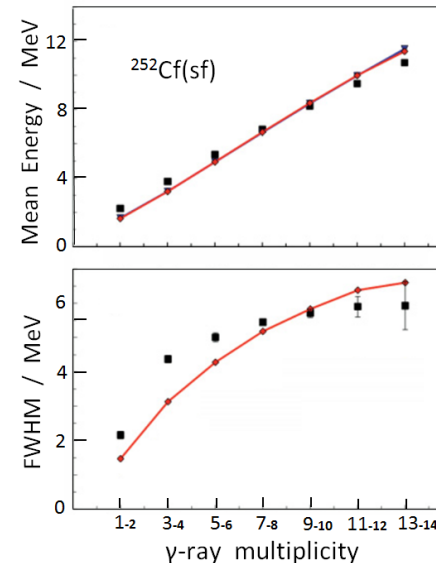
The total gamma energy E_γ increases linearly with the multiplicity. This tells that up to the highest multiplicities the average photon energy remains constant.

By contrast, the FWHM is leveling off.

Chyz 2012

Gamma energy E_γ and multiplicity M_γ of photons as a function of fragment masses was investigated for several standard (n_{th},f) and (sf) reactions. A typical example is on display for $^{239}Pu(n_{th},f)$. For a time window of less than 5 ns
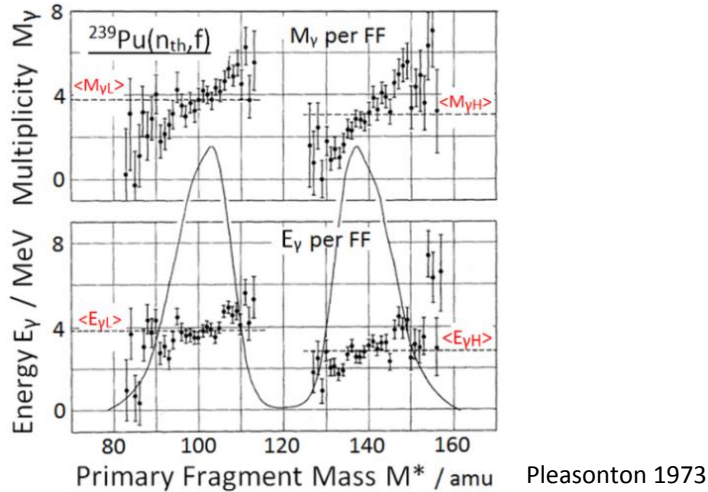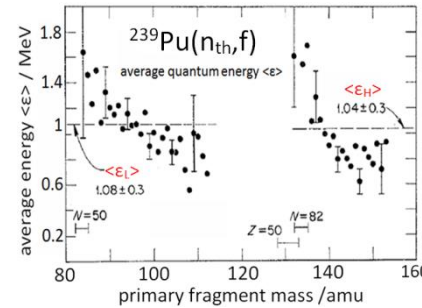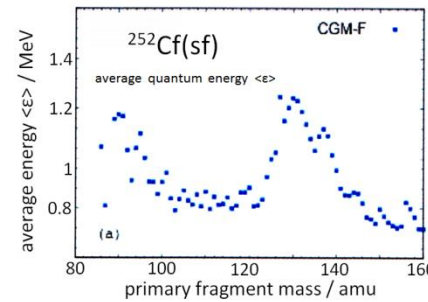

Pleasonton 1973

the multiplicity M_γ has the same sawtooth behaviour as the neutron multiplicity ν_n. Likewise the total average gamma energies $<E_\gamma>$ per FF follow in shape a sawtooth vs. fragment mass. For the reaction $^{252}Cf(sf)$ see [Nardi 1973].

The saw-tooth shapes of multiplicity versus fragment mass are similar for both, neutrons and gammas. They have in fact as a common root the deformation of fragments at scission. For neutrons it is the large energy stored in the large deformation which is counting while for gammas large deformations lead to large angular momenta of fragments having to be exhausted by more than average numbers of photons.

In contrast to the average multiplicity vs. fragment mass the plot of the average quantum energy $<\varepsilon>$ vs. fragment mass looks like an anti-saw-tooth. For magic fragments the γ-multiplicity is low but the quantum energy $<\varepsilon>$ is large.

This is due to the widely spaced energy levels for these nuclei.

Experiment $^{239}Pu(n_{th},f)$:
In contrast to γ-multiplicity M_γ or total γ-energy E_γ the average quantum energies $<\varepsilon(A)>$ are large for cluster nuclei with $N = 50$ in the light and $(Z = 50, N = 82)$ in the heavy group.

Pleasonton 1973

The actinide targets ^{233}U, ^{235}U and ^{239}Pu studied in thermal neutron fission and (sf) of ^{252}Cf exhibit similar features for $<\varepsilon(A)>$. As shown for $^{252}Cf(sf)$ theory describes well the structure of $<\varepsilon(A)>$ versus fragment mass A.

Talou 2013

Peculiarities for magic fragments

The γ-spectra for virtually all fragments are very similar. There is, however, an exception for magic fragments. For example in
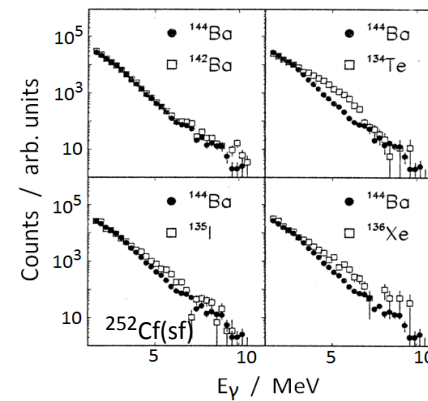
Biswas 1999

$^{252}Cf(sf)$ these nuclei exhibit an enhancement of γ-yield at energies ε_γ near 5 MeV. This is attributed to the wider spacing of levels in magic nuclei. At given excitation energy this will favor the emission of hard photons.

Anisotropy of Gamma Emission

Very early in the history of fission it was discovered that the emission of gammas is non-isotropic relative to the fission axis.

Skarsvag 1980
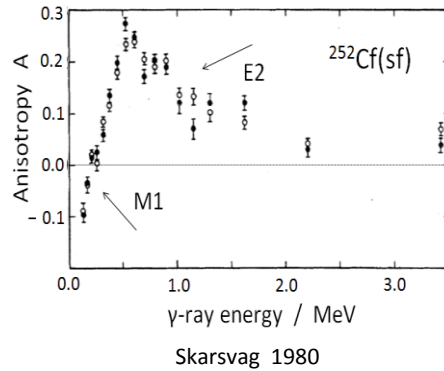
This was found for all low energy fission reactions studied. An example is shown in the figure for ^{252}Cf(sf). The anisotropy A is defined as
$$A = [W(0°)–W(90°)]/W(90°)$$
for the angle $\theta_{\gamma f}$ between the gamma and the fi-axis.

The anisotropy measured varies strongly with γ-energy. For low-energy gammas with $E_\gamma < 200$ keV the anisotropy A is A < 0 with more gammas emitted at θ = 90° perpendicular to the fission axis than along the fission axis at θ = 0°. The anisotropy changes sign for the majority of gammas with energies $E_\gamma > 200$ keV. For positive A > 0 gammas are preferentially emitted along the fission axis.

A succinct interpretation of the anisotropy was given by V. Strutinski in 1960. It is pointed out that the sizable angular momenta carried by the fragments are oriented in a plane perpendicular to the fission axis. The probability for emission of gammas is a function of the angle $\theta_{\gamma I}$ between the gamma and fragment spin I. After averaging over all orientations of spin around the fission axis the angular distribution W(θ) becomes a function of the angle $\theta_{\gamma f}$ between the gamma and the fission axis in the CM system of the fragment. To each multipole L of the radiation field thereby belongs a characteristic angular emission pattern.

According to Strutinski the angular distribution $W(\theta_{\gamma I})$ of gammas relative to fragment spin I reads
$$W_{L=1}(\theta_{\gamma I}) \approx 1 + \tfrac{1}{4}(\hbar^2 J/\Im\, T)^2 \cos^2 \theta_{\gamma I} \text{ for L = 1 (dipole) and}$$
$$W_{L=2}(\theta_{\gamma I}) \approx 1 – \tfrac{3}{4}(\hbar^2 J/\Im\, T)^2 \cos^2 \theta_{\gamma I} \text{ for L = 2 (quadrupole)}$$
with $\Im$ the moment of inertia and T the temperature. The already mentioned averaging over the orientations of I may be shown to yield
$$<\cos^2\theta_{\gamma I}> = \tfrac{1}{2} \sin^2\theta.$$
The angular distributions $W_L(\theta_{\gamma f})$ relative to the fission axis are
$$W_{L=1}(\theta_{\gamma f}) \approx 1 + \tfrac{1}{8}(\hbar^2 I/\Im\, T)^2 \sin^2 \theta_{\gamma f} \text{ for L = 1 (dipole) and}$$
$$W_{L=2}(\theta_{\gamma f}) \approx 1 – \tfrac{3}{8}(\hbar^2 I/\Im\, T)^2 \sin^2 \theta_{\gamma f} \text{ for L = 2 (quadrupole).}$$

Note that the anisotropy A is negative for dipole and positive for quadrupole gammas. This could explicitly be verified by studying the anisotropy for single transitions between known levels in the ^{252}Cf(sf) reaction as shown in the figure. To the

Wilhelmy 1972
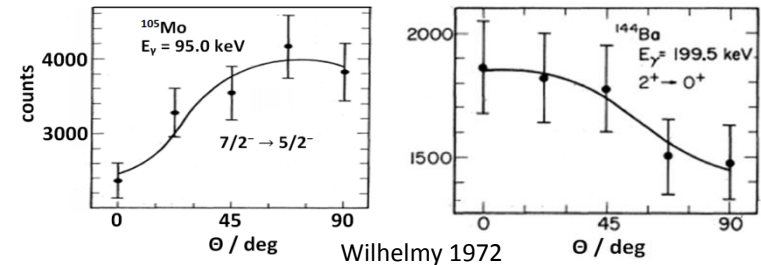
left the M1 dipole gammas to the groundstate of ^{105}Mo are preferentially emitted perpendicular to the fission axis, while the E2 quadrupole gammas to the groundstate of ^{144}Ba favor emission along the fission axis. It has to be pointed out that the above angular distribution from theory pertain to the emission in the CM system of fragments while the experimental results are obtained in the LAB system. Yet the transformation from the CM to the LAB system will not change the characteristics of the angular distributions.

To measure extremely short emission half-lives of gammas from fragments require special techniques. Two ingenious methods have been devised. In a **first method** the high velocity V of fission fragments of about V ≈ 1 cm/ns is exploi-

^{252}Cf(sf)

Relative Intensity

Emission Time / 10^{-10} s

Johansson 1964
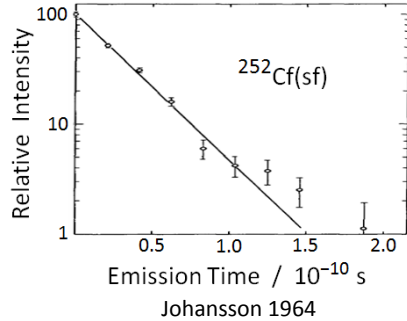
ted. Scanning along the vacuum flight path the γ`s emitted perpendicular to the path, the fastest γ`s are emitted closest to the source while for increasing half-lifes the gammas are appearing farer and farer away from the source. At about 1 cm of flight path gammas with life times of 1 ns are expected to be seen. Scanning gammas with a collimator along the fragment path with a definition of 0.1 mm, decay times down to 10^{-11}s have been assessed. In the figure the decay of the gamma intensity for ^{252}Cf(sf) is found to be exponential with a half-life of 2.3 $\cdot 10^{-11}$s. There is, however, a tailing for longer emission times.

A **second method** relies on the angular aberration of gammas emitted in flight from a moving fragment. Let θ be the angle in the fragment system CM between the direction of gamma emission relative to the velocity vector of the light fragment , and ϑ the angle in the LAB system. Then the relativistic transformation of coordinates yields

$$\tan\theta = (1-\beta^2)^{\frac{1}{2}}\sin\vartheta \, / \, (\cos\vartheta - \beta) \quad \text{with } \beta = V/c$$

and V the fragment velocity. For all CM angles θ the LAB angles ϑ are smaller than θ. In the forward direction (ϑ near 0°) the gammas are in the LAB hence squeezed into a narrower cone, while in the backward direction (ϑ near 180°) they are diluted in a wider cone. From the condition

$$W_{CM}(\theta)\sin\theta d\theta = W_{LAB}(\vartheta)\sin\vartheta d\vartheta$$

the transformation law for angular distributions becomes

$$W_{LAB}(\vartheta) = W_{CM}(\theta)\{(1-\beta^2)/(1-\beta\cos\theta)^2\}$$

A forward–backward anisotropy $A_{fb} \sim [W_{LAB}(0°)-W_{LAB}(180°)] \neq 0$ shows up for β ≠ 0 in the lab which is due to the cosθ term (note that in the CM system of fragments or for fragments at rest there is no fb anisotropy).
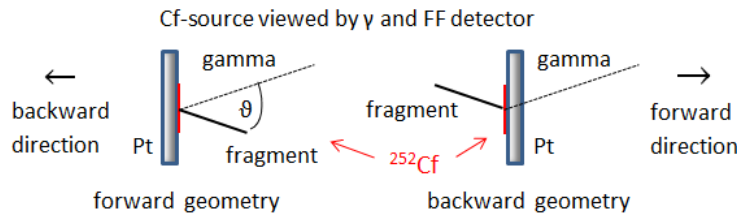
The above angular aberration of gammas is evidently similar to the anisotropic emission of neutrons observed in the lab. However, for gammas the anisotropy is much less pronounced than for neutrons and this makes it difficult to disentangle the contributions to the anisotropy A_{fb} from the two complementary fragments. So far it has only been feasible to distinguish between average contributions from the light and heavy group by manipulating the fb anisotropy.

The idea is to compare angular aberrations from gammas emitted by un-slowed fragments travelling in vacuum to gammas emitted from fragments being slowed down in a dense material. The stopping times of fragments in dense matter are very short. In platinum $V(t) = V_0\exp{-t/\alpha}$ with α = 0.5 ps. These short stopping times have the same order of magnitude as the emission times of gammas from fragments. In the limiting case of very early gammas ($T_{\frac{1}{2}} \ll \alpha$) the fb anisotropy observed in the lab remains the same whether fragments are slowed down or not. This situation obtains for neutron evaporation from fragments whence it is concluded that neutrons are emitted in times shorter than a few 10^{-14} s. By contrast, in the limit of very late gammas with $T_{\frac{1}{2}} \gg \alpha$ the fb anisotropy in the lab vanishes altogether because fragments have been stopped before gammas are emitted. In the general case the fb anisotropy yields information on gamma emission times relative to stopping times.

The layout of experiments performed by Skarsvag (1964-1980) measuring angular aberrations of gammas is discussed in the following.

The layout of experiments to measure angular aberrations of gammas as proposed by Skarsvag [Skarsvag 1964] is sketched in the figure. A thin ^{252}Cf(sf) fission source on a platinum backing just thick enough to stop fragments is mounted in a vacuum chamber. One of the fragment is stopped in the backing while the complementary fragment is ejected into vacuum. Coincidences between gammas and fragments ejected are taken in two different geometries. In the "forward" geometry both the gamma and the

Cf-source viewed by γ and FF detector

gamma

backward direction   Pt   fragment   ϑ   fragment ^{252}Cf   Pt   forward direction

gamma

forward geometry   backward geometry

fragment detector are facing the front side of the source while in the "backward" geometry the gammas are detected from the back side and the fragment from the front side of the Pt backing. The gamma detector sees the γ`s from both fragments simultaneously, from the one moving freely into vacuum and from the one being slowed down in the backing. In the forward geometry the γ-detector senses un-slowed in the forward and slowed down FF in the backward direction and vice versa for the backward geometry. Since only one of the fragments is intercepted it is merely possible to distinguish between fragments belonging either to the light or the heavy fragment group.

The γ-energy was divided into 12 windows from ε_γ = 0.10 MeV up to ε_γ = 2.57 MeV and beyond. From the four data sets for the two geometries and the two types of fragments (LF and HF) the gamma intensities and the angular aberrations were evaluated for each of the γ-energy windows. The angular aberrations yield the velocity β = V/c at the time of γ-emission. By comparing β with the time dependent β(t) of the stopping law the time of γ-emission is found.

In the evaluation the Doppler shift of photon energy,
$$E_{LAB} = E_{CM}(1+\beta\cos\vartheta),$$
with E_{lab} and E_{cm} the energy in the LAB and CM system of fragments, and the velocity dependence of the solid angle seen by the fragment moving at velocity β have in addition to be taken into account.
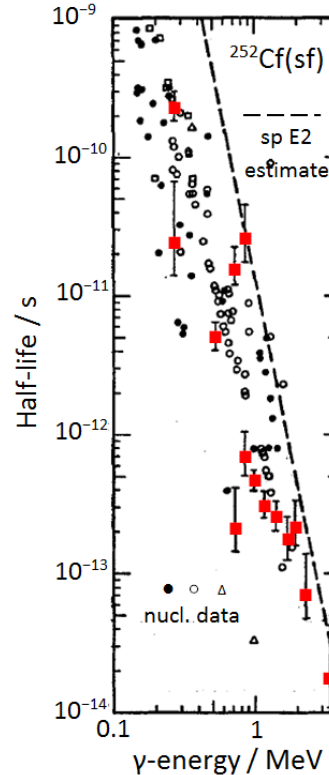
The results obtained by the aberration method are impressive. They are shown in the figure as squares with experimental error bars. Half-lifes for γ- emission ranging from 1 ns to times as short as 10^{-14}s are assessed. The earliest γ`s with $T_{1/2} < 10^{-12}$ s have the highest energies in excess of 1 MeV while gammas with energies below 1 MeV are emitted in times longer than 10^{-12} s. Since the first gammas take away large amounts of energy, half of the total γ-energy is exhausted in the short time of $T_{1/2} < 4\cdot10^{-13}$ s .

Skarsvag 1975

Large E_γ are due to E2 transitions (see foil 21). The dashed line in the figure is the single-particle estimate for E2 transitions. The experimental data point to much faster E2 transitions in fission. They must hence be collective in nature. Samples of half-lifes from nuclear data tables (not necessarily fission fragments) are included for comparison.

Evolution in emission time

of total gamma energy and gamma multiplicity.

Summarizing the discussion of emission times of gammas the figure displays the evolution in time separately for gamma energy E_γ and gamma multiplicity M_γ.

Skarsvag 1975
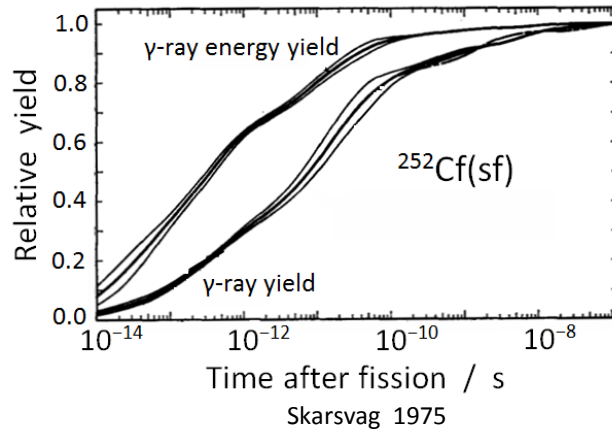
The experimental results shown were obtained for the reaction ^{252}Cf(sf). They should be typical for low energy fission of actinides.

The earliest gammas appear at about 10^{-14} s after scission. The bulk of prompt gammas is emitted within 100 ns. Late but still prompt gammas emitted by fragments are found in times up to about 1 ms. In the particular case of fission isomers even longer times may be observed. Yet after about 1 ms β-decay of fragments is starting. The daughter products are a copious source of delayed gammas.

In the above figure it is noteworthy that the total photon energy increases faster with time than the total number of photons. This just reflects the fact that early gammas have higher energies.

Competition n ⟷ γ Emission

Already in 1952 J.S. Fraser established an upper limit of $4 \cdot 10^{-14}$ s for the time of neutron emission. The reactions studied were thermal neutron induced fission of U- and Pu- isotopes.

Comparing neutron and gamma emission it becomes evident that at about 10^{-14} s after fission the last neutrons and the first gammas may appear simultaneously. There is hence a competition between neutron and gamma emission.

In experiment this competition is observed as a positive correlation between total γ-ray energy and total neutron multiplicity. The correlation between average γ-energy $<E_\gamma>$ and qverage neutron multiplicity $<v>$ is on display in the figure for the reaction ^{252}Cf(sf). The interpretation of the positive correlation has been given by Johansson [1964] :

Nifenecker 1972
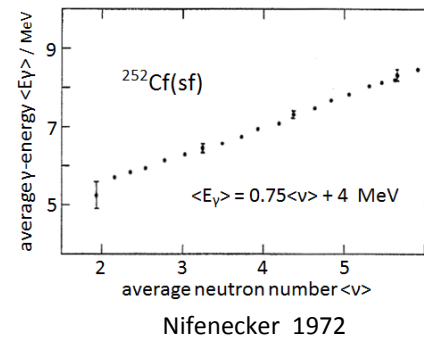
The n ↔ γ competition is in particular effective for fragments excited to high spin states. Neutrons drain efficiently excitation energy but not angular momentum. Near the end of the neutron cascade the excitation has hence become small but the spin may still be large. Level densities at low energy but high spin are low and neutron evaporation to final states in the daughter nucleus is delayed. This gives gammas a better chance to compete and to exhaust the remaining angular momentum. This leads to the positive correlation observed.

Late Gammas

Gammas emitted in times > 50 ns after scission may be called "late" gammas. They should not be confounded with β-delayed gammas emitted following β-decay by daughter nuclei left in an excited state. These are responsible for the long-lasting radioactivity of waste from nuclear power stations. By contrast, late gammas presently to be discussed stem from isomeric states of fragments having been excited in the course of fission.

Searching for late gammas, in a study of spontaneous fission of ^{252}Cf the time window of γ-detection was extended from 3 ns to 2000 ns. The figure due to W. John (1970) shows γ-spectra in the time range 10 ns to 2000 ns. Remarkably, long-living isomers, albeit with small yields, show up for two different ranges of γ-energy: for low energies below 500 keV and for very high energies near 1250 keV. It is further found that these γ`s are preferentially emitted from fragments near mass 132. This mass number suggests the influence of magic shells like in ^{132}Sn. Microsecond isomers in the magic regions ^{78}Ni and ^{132}Sn have been extensively studied in recent years [Pinston 2004].

John 1970
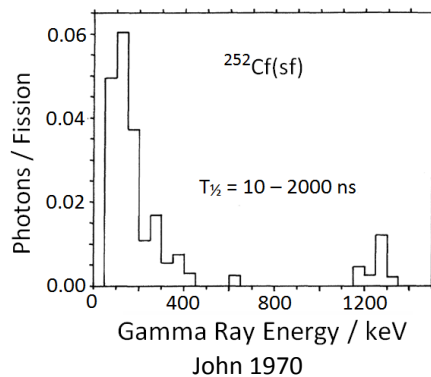
From the γ-anisotropy measurements discussed in the foregoing it is concluded that these high energy gammas have the multipolarity E2. They may possibly be interpreted as collective vibrations of stiff magic nuclei. However, they are by orders of magnitudes slower than anticipated. Most probably this tells that the quanta in question are fed by γ-cascades with a long-living spin isomer on top of the cascade.

Concluding remarks

Only a few weeks after the discovery of nuclear fission, a report on the observation of fission neutrons was published in the issue of March 1939 of "Nature"[von Halban 1939]. Since that time the properties of neutrons from fission have been intensely studied. Consistent sets of experimental data have been evaluated and published [nndc.bnl.gov]. As to theory the situation is less favorable. Though it is generally accepted that the majority of neutrons are evaporated from fully accelerated fission fragments, it is evident from experiment that there are still other sources like scission neutrons contributing. A very probable mechanism for their creation is the excitation of neutron states in the non-adiabatic rupture of the neck joining the two nascent fragments. These states decay by neutron emission into the vacuum. Energies and angular distributions of these neutrons are discussed controversially. A further issue concerns the impact of anisotropic neutron emission in the CM system of the fragments on energy spectra and angular distributions

As a rule neutron emission is followed by gamma emission. In comparison to neutrons the properties of fission gammas have been much less investigated. In part this is due to the experimental difficulties linked to the wide ranges of gamma energies and time distributions. For gammas even such basic quantities as average multiplicity $<M_\gamma>$ or total gamma energy $<E_\gamma>$ are not known with the accuracy which should in principle be accessible nowadays. For example, even for the best studied reactions, ^{235}U(n_{th},f) and ^{252}Cf(sf), the total gamma energy release E_γ quoted by different authors differ by more than 1 MeV, a difference of ≈15%. Recently gamma emission has found revived interest and the situation should improve.

References "Neutron Emission"

H.R. Bowman et al.: Phys. Rev. 126 (1962) 2120 and
   Phys. Rev. 129 (1963) 2133
U. Brosa, S. Grossmann and A. Müller: Phys. Reports 197 (1990) 167
C. Budtz-Jørgensen and H.H. Knitter.: Nucl. Phys. A490 (1988) 307
V.E. Bunakov , I. Guseva, S.G. Kadmenski and G. A. Petrov: Proc.
   "Interactions of Neutrons with Nuclei", Dubna 2006, p293
N. Carjan et al.: Phys. Rev. C82, 014617 (2010)
T. Ericson and V. Strutinski, Nucl. Phys. 8, 284 (1958)
T. Ethvignot et al.: Phys. Rev. Lett. 94, 052701 (2005)
C.B. Franklyn et al.: Phys. Lett. 78B (1978) 564
J.S. Fraser: Phys. Rev. 88, 536 (1952)
J. Fréhaut : Proc. "Nuclear data for Science and Technology",
   Mito Conf. 1988, IAEA 1989, p81
R.W. Fuller: Phys. Rev. 126, 648 (1962)
A.M. Gagarski et al.: Proc. "Interactions of Neutrons with Nuclei",
   Dubna 2012, http://isinn.jinr.ru/isinn20
I. Guseva : private communication 2014
O. Hahn and F. Strassmann: Naturwiss. 27, 89 (1939)
H. von Halban, F. Joliot and L. Kowalski: Nature 143, 470 (1939)
I. Halpern: Proc. "Physics and Chemistry of Fission"
   IAEA, Vienna, 1965, Vol. II, p369
D. Hilscher and H. Rossner: Ann. Phys.(Paris), 17 (1992) 471

D.C. Hoffman et al. "Nuclear Decay Modes", IOP Publishing , 1996, p393
O. Litaize and O. Serot: Phys. Rev. 82, 054616 (2010)
W. Mannhart: IAEA, TECDOC 410, 1987 p158
D. G. Madland: Proc. "50 Years with Nuclear Fission", Am. Nucl. Soc. 1989,
   Vol I, p 429
E.E. Maslin, A. L. Rodgers, W.G.F. Core: Phys. Rev. 164, 1520 (1967)
R. Müller, A.A. Naqvi, F. Käppeler and F. Dickmann: Phys. Rev. C 29, 885 (1984)
K. Nishio, Y. Nakagome et al.: Nucl. Phys. A 632, 540 (1998)
H. W. Schmitt, J.H. Neiler and F.J. Walter: Phys. Rev. 141, 1146(1966)
C. Signarbieux et al.: Phys. Lett. 39B, 503 (1972)
K. Skarsvag and K. Bergheim: Nucl. Phys. A , 72 (1963)
P. Talou et al.: Phys. Rev. C 83, 064612 (2011) and
   Phys. Proc. 47, 39 (2013)
J. Terrell: Phys. Rev. 108, 783 (1957) and Phys. Rev. 113, 527 (1959
R. Vandenbosch and J.R. Huizenga : "Nuclear Fission" , Academic Press, 1973
R. Vogt and J. Randrup: Phys. Rev. C 80, 044611 (2009)
A.S. Vorobyev et al.: Proc. "Interactions of Neutrons with Nuclei",
   Dubna 2001, p276 and Dubna 2009, p60
R.L. Walsh et al.: Nucl. Phys. A276 (1977) 189
V. P. Zakharova et al.: Sov. J. Nucl. Phys. 30 (1979) 19
Sh. Zeynalov et al.: Proc. "Nuclear Fission and Fission-Product
   Spectroscopy", AIP Conf. Proc. 1175, p359 (2009)

References "Gamma Emission"

B. Becker, P. Talou et al: Phys. Rev. 87, 014617 (2013)
D.C. Biswas, B.K. Nayak et al.: Eur. Phys. J. A4, 343 (1999)
R. Billnert, F.-J. Hambsch et al: Phys. Rev. C 87, 024601 (2013)
A. Chyzh, C.Y. Wu, E. Kwan et al.: Phys. Rev. C85, 021601 (2012)
A. Chyzh, C. Y. Wu, E. Kwan et al: Phys. Rev. C 87, 034620 (2013)
J. Fréhaut: IAEA report, INDC (NDS) -220, 1989, p 99
S.A.E. Johansson: Nucl. Phys. 60, 378 (1964)
W. John, F.W. Guy and J.J. Wesolowski: Phys. Rev. C 2, 1451 (1970)
H.-H. Knitter, U. Brosa and C. Budtz-Jørgensen: in "The Nuclear Fission
   Process", C. Wagemans ed., CRC Press 1991, p 497
E. Nardi, A. Gavron and Z. Fraenkel: Phys. Rev. 8, 2293 (1973)

H. Nifenecker, C. Signarbieux, M. Ribrag et al: Nucl. Phys. A 189, 285
   (1972)
A. Oberstedt, T. Belgya et al: Phys. Rev. C 87, 051602(R) (2013)
F. Pleasonton: Phys. Rev. 6, 1023 (1972)
F. Pleasonton: Nucl. Phys. A 213, 413 (1973)
K. Skarsvag and I. Singstad: Nucl. Phys. 62, 103 (1965)
K. Skarsvag: Nucl. Phys. 253, 274 (1975)
K. Skarsvag: Phys. Rev. C 22, 638 (1980)
P. Talou, T. Kanon and I. Stet: Phys. Proc. 47, 39 (2013)
V.V. Verbinski, H. Weber and R.E. Sund: Phys. Rev. C 7, 1173 (1973)
R. Vogt and J. Randrup: Phys. Rev. C 84, 044621 (2011)
J.B. Wilhelmy, E. Cheifetz, J.R.C. Jared et al : Phys. Rev. C 5, 2041 (1972)